Loss of the scavenger receptor MARCO results in uncontrolled vomocytosis of fungi from macrophages

Onyishi, Chinaemerem U.; Jeon, Yusun; Fejer, Gyorgy; Mukhopadhyay, Subhankar; Gordon, Siamon; May, Robin C.

DOI:
10.1002/eji.202350771

European Journal of Immunology
Clinical·Basic·Translational

Innate immunity

Basic

Short Communication

Loss of the scavenger receptor MARCO results in uncontrolled vomocytosis of fungi from macrophages

***Chinaemerem U. Onyishi*[1,2], *Yusun Jeon*[3], *Gyorgy Fejer*[4], *Subhankar Mukhopadhyay*[3], *Siamon Gordon*[5,6] and *Robin C. May*[1]**

[1] Institute of Microbiology & Infection and School of Biosciences, University of Birmingham, Edgbaston, Birmingham, UK
[2] Molecular Mycology and Immunity Section, Laboratory of Host Immunity and Microbiome, National Institute of Allergy and Infectious Diseases (NIAID), National Institutes of Health, Bethesda, MD, USA
[3] Peter Gorer Department of Immunobiology, School of Immunology & Microbial Sciences, King's College London, London, UK
[4] School of Biomedical Sciences, Faculty of Health, University of Plymouth, Plymouth, UK
[5] Department of Microbiology and Immunology, College of Medicine, Chang Gung University, Taoyuan, Taiwan
[6] Sir William Dunn School of Pathology, University of Oxford, Oxford, UK

Vomocytosis, also known as nonlytic exocytosis, is a process whereby fully phagocytosed microbes are expelled from phagocytes without discernible damage to either the phagocyte or microbe. Although this phenomenon was first described in the opportunistic fungal pathogen *Cryptococcus neoformans* in 2006, to date, mechanistic studies have been hampered by an inability to reliably stimulate or inhibit vomocytosis. Here we present the fortuitous discovery that macrophages lacking the scavenger receptor MAcrophage Receptor with COllagenous domain (MARCO), exhibit near-total vomocytosis of internalised cryptococci within a few hours of infection. *Marco*$^{-/-}$ macrophages also showed elevated vomocytosis of a yeast-locked *C. albicans* strain, suggesting this to be a broadly relevant observation. We go on to show that MARCO's role in modulating vomocytosis is independent of its role as a phagocytic receptor, suggesting that this protein may play an important and hitherto unrecognised role in modulating macrophage behaviour.

Keywords: Cryptococcus · Fungal pathogen · Innate immunity · Macrophage · MARCO · Vomocytosis

Additional supporting information may be found online in the Supporting Information section at the end of the article.

Introduction

Cryptococcus neoformans is an opportunist fungal pathogen that causes life-threatening meningitis, mainly in immunocompromised individuals such as HIV/AIDS patients [1]. Infection is thought to begin with the inhalation of the fungi into the lungs where it encounters macrophages of the innate immune system that serve as the first line of defence against infection [1]. The interaction between *C. neoformans* and macrophages can lead to a range of outcomes including fungal survival and replication within macrophages [2], lateral transfer of cryptococci between

Correspondence: Dr. Chinaemerem U. Onyishi and Prof. Robin C. May
e-mail: chinaemerem.onyishi@nih.gov; r.c.may@bham.ac.uk

macrophages [3, 4], lysis of macrophages [5], and vomocytosis, also called nonlytic exocytosis [6, 7].

Vomocytosis is a nonlytic expulsion mechanism where fully phagocytosed fungi are expelled from the macrophage with no evidence of host cell damage [6–8]. Vomocytosis occurs through the fusion of *Cryptococcus*-containing phagosome with the plasma membrane in a manner that is modulated by the actin cytoskeleton [9]. It has also been shown to require phagosome membrane permeabilization [9] and a failure to fully acidify the phagosome [10, 11]. Previous studies have identified the mitogen-activated protein kinase ERK5 and the phospholipid-binding protein Annexin A2 (ANXA2) as regulators of vomocytosis, with ERK5 inhibition and ANXA2-deficiency leading to increased and decreased vomocytosis, respectively [12, 13]. Moreover, stimulation of macrophages with type 1 interferons (IFN-α and IFN-β), mimicking viral coinfection, increased cryptococcal vomocytosis [14]. Very little else is known about the host regulators of vomocytosis.

Here we present the chance observation that the scavenger receptor MAcrophage Receptor with Collagenous structure (MARCO) is a key modulator of vomocytosis. Typically, vomocytosis rates from wildtype macrophages are between 10–20%, but this number rises close to 100% in *Marco*$^{-/-}$ macrophages. Further investigation indicates that this impact on vomocytosis is likely independent of MARCO's role in phagocytosis. As well as providing a powerful experimental tool for future investigations into this phenomenon, this finding also has important implications for interpreting infection assays conducted in *Marco*$^{-/-}$ animals.

Results and discussion

Marco$^{-/-}$ macrophages show increased vomocytosis of non-opsonised *C. neoformans*

While investigating the role of scavenger receptors in the phagocytosis of *C. neoformans* using a non-transformed GM-CSF dependent alveolar-like macrophage cell line derived from wildtype and *Marco*$^{-/-}$ C57BL/6 mice [15], we observed that, in LPS-stimulated macrophages, MARCO-deficiency led to decreased non-opsonic phagocytosis of *C. neoformans* (Fig. 1A). Using live cell imaging to observe the interaction between *C. neoformans* and macrophages after the initial 2 h of infection, we noted a dramatic increase in the vomocytosis of *C. neoformans* from *Marco*$^{-/-}$ macrophages, with 80–100% of infected macrophages experiencing at least one vomocytosis event (Fig. 1B; Supporting information Video S1). No other host or pathogen factor has been found to increase the rate of vomocytosis to such an extent. Not only did *Marco*$^{-/-}$ macrophages show elevated vomocytosis, but 75% of nonlytic expulsion events occurred within the first 1 h 40 min of the initiation of the timelapse video (note timelapse videos began after *C. neoformans* was incubated with macrophages for 2 h to allow for phagocytosis), with the median time to a vomocytosis event being 0.92 h (55 min; Fig. 1C; Supporting information Video S2). In contrast, vomocytosis in wildtype macrophages occurred over a wider range of time with the median time to vomocytosis being 10.6 h (10 h:35 min; Fig. 1C). We also observed elevated vomocytosis in unstimulated *Marco*$^{-/-}$ macrophages, though to a lesser extent than LPS-stimulated macrophages, suggesting the mechanism of action is somewhat dependent on macrophage stimulation state (Fig. 1D).

Table 1. Quantification of the vomocytosis of heat-killed *C. neoformans* in wildtype and *Marco*$^{-/-}$ macrophages.

	Total number of macrophages counted	Number of infected macrophages counted	Number of vomocytosis events observed
Wildtype	760	39	0
Marco$^{-/-}$	709	16	0

To follow the interaction between *C. neoformans* and macrophage from phagocytosis through to nonlytic expulsion, timelapse imaging was carried out immediately following macrophage incubation with *C. neoformans*. There was no difference in the time to phagocytosis between wildtype (n = 48) and *Marco*$^{-/-}$ (n = 67) macrophages. Most phagocytosis occurred within the first 90 minutes with only two phagocytosis events being observed after 2 h incubation (Fig. 1E). During this extended imaging, we observed only three vomocytosis events from wildtype macrophages, all of which were beyond the initial 2 h incubation (Fig. 1F). In contrast, we observed 51 vomocytosis events out of 67 infected *Marco*$^{-/-}$ cells, with 9 out of 51 happening before 2 h (Fig. 1F). This provides further evidence that vomocytosis from *Marco*$^{-/-}$ macrophages is both abundant and rapid. It also suggests that the rate of non-lytic expulsion events from *Marco*$^{-/-}$ cells is underestimated in Fig. 1B and C since, in these experiments, timelapse imaging began only 2 h after infection. Fig. 1F provides a representative image of non-opsonised *C. neoformans* being expelled from *Marco*$^{-/-}$ macrophages.

MARCO deficiency leads to elevated vomocytosis of 18B7 antibody-opsonised *C. neoformans* and yeast-locked *Candida albicans*, but not heat-killed *C. neoformans* or latex beads

To investigate the generality of this phenomenon, we infected macrophages with heat-killed *C. neoformans*, 7 μm diameter latex beads, anti-GXM 18B7 antibody-opsonised *C. neoformans*, and a yeast-locked TetOn-NRG1 *C. albicans* strain that constitutively expresses Nrg1 transcription factor, thereby preventing yeast-to-hypha formation [16]. In line with previous data showing that inert particles do not undergo vomocytosis [6, 7], we observed no vomocytosis of heat-killed *C. neoformans* by either wildtype or *Marco*$^{-/-}$ macrophages out of 55 infected macrophages observed (Table 1), and only a single event (amongst 239 infected cells) when macrophages were "infected" with latex beads (Table 2). Notably, *Marco*$^{-/-}$ macrophages showed decreased phagocy-

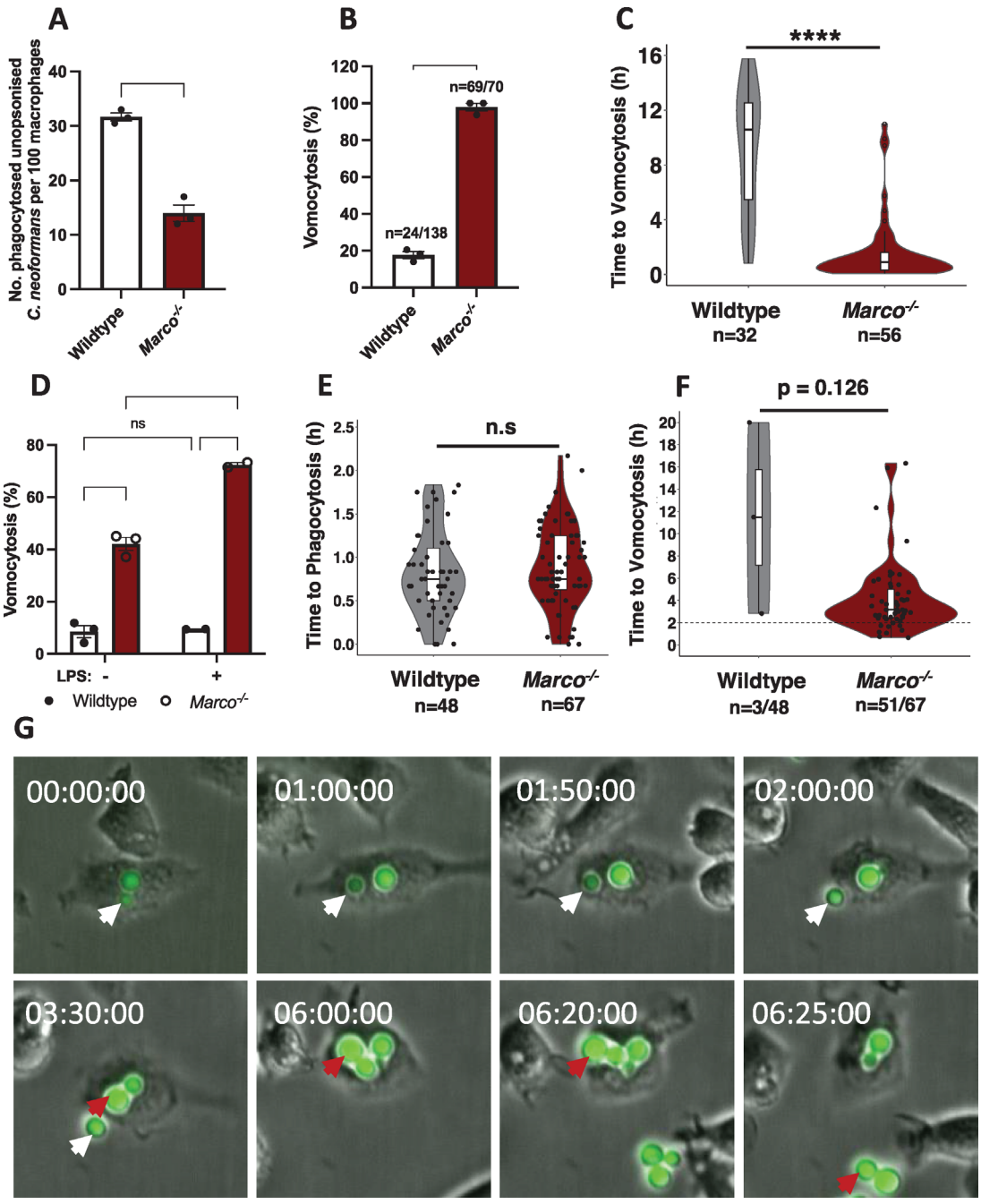

Figure 1. Macrophages were unstimulated or stimulated overnight with LPS and then infected with non-opsonised *Cryptococcus neoformans*. Time-lapse imaging began 2 h postinfection (A-D and G). (A) Phagocytosis was quantified 2 h postinfection (beginning of timelapse) as the number of internalised cryptococci per 100 macrophages. (B) Vomocytosis was quantified over a 16 h period and presented as the percentage of infected macrophages that experienced one or more vomocytosis events. At least 200 macrophages were observed. Wildtype: $n = 24$ vomocytosis events out of 138 infected macrophages; *Marco*$^{-/-}$: $n = 69$ vomocytosis events out of 70 infected macrophages. (C) The time at which individual vomocytosis events took place was quantified and expressed as decimals. Wildtype ($n = 32$ vomocytosis events); *Marco*$^{-/-}$ ($n = 56$ vomocytosis events). A violin plot with an overlapping box plot was created using the ggplot2 package on R. (D) Vomocytosis in LPS unstimulated and stimulated macrophages. (E, F) Timelapse imaging began immediately after non-opsonised *C. neoformans* incubation with macrophages at MOI 0.5:1. (E) The time at which individual phagocytosis events occurred. Wildtype ($n = 48$); (*Marco*$^{-/-}$ $n = 67$). (F) The time at which individual vomocytosis events took place. Wildtype: $n = 3$ vomocytosis events out of 48 infected macrophages); *Marco*$^{-/-}$: $n = 51$ vomocytosis events out of 67 infected macrophages. The dashed line at 2 h timepoint highlights the time by which most phagocytosis events would have taken place. Data is presented as mean ± SEM; n.s., not significant, $^{***}p < 0.001$, $^{****}p < 0.0001$ in an unpaired two-sided *t*-test (A, B), two-way ANOVA followed by Tukey's post hoc test (D) and Mann–Whitney *U* test (C, E, F). Data is representative of at least two independent experiments. (G) Representative image showing vomocytosis of GFP-expressing *C. neoformans* from *Marco*$^{-/-}$ macrophages. Time is presented in hh:mm:ss; white and red arrows follow the course of expulsion events.

Table 2. Quantification of the vomocytosis of latex beads in wildtype and *Marco*$^{-/-}$ macrophages.

	Total number of macrophages counted	Number of infected macrophages counted	Number of vomocytosis events observed
Wildtype	2477	203	1
Marco$^{-/-}$	2456	36	0

tosis of heat-killed cryptococci and latex beads compared to wildtype cells, hence the lower numbers of infected *Marco*$^{-/-}$ macrophages.

Next, macrophages were infected with antibody-opsonised fungi to drive uptake via FcγRs. As expected, there was no difference in antibody-opsonised phagocytosis between wildtype and *Marco*$^{-/-}$ macrophages (Fig. 2A). However, vomocytosis was elevated in *Marco*$^{-/-}$ macrophages compared with wildtype cells (Fig. 2B). Finally, macrophages were infected with a yeast-locked *C. albicans* strain that fails to undergo filamentation and then observed for 6 h. In this experiment, timelapse imaging began immediately following macrophage incubation with *Candida*. As expected, since phagocytosis of *Candida* is predominantly driven by Dectin-1 [17], there was no difference in phagocytosis between wildtype and *Marco*$^{-/-}$ macrophages (Fig. 2C). Surprisingly, we observed increased vomocytosis of yeast-locked *Candida* from MARCO-deficient macrophages (Fig. 2D and E; Supporting information Video S3). The percentage of *Marco*$^{-/-}$ macrophages that experienced at least one vomocytosis event was not as dramatic as that observed with *Cryptococcus*; however, vomocytosis of wildtype *C. albicans* is rare, happening at a rate of <1% over a 6-hour period [18]. Therefore, a rate of 30% over 6 hours in *Marco*$^{-/-}$ cells is significant for this fungal pathogen. Given that elevated vomocytosis was observed when phagocytosis was mediated by non-opsonic receptors (Fig. 1B), FcγR (Fig. 2B), and Dectin-1 (Fig. 2D), it seems likely that the role of MARCO in vomocytosis is independent of the mechanism of uptake.

Treatment of wildtype MPI cells with inhibitors of MARCO does not phenocopy increased vomocytosis seen in *Marco*$^{-/-}$ cells

To explore whether the vomocytosis phenotype seen in *Marco*$^{-/-}$ can be induced in wildtype macrophages, we exposed wildtype cells to polyguanylic acid potassium salt (polyG), a MARCO ligand and inhibitor [19], and quantified vomocytosis. Like the genetic knockout of *MARCO*, polyG pre-treatment also decreased the phagocytosis of non-opsonised *C. neoformans* (Fig. 2F). However, the inhibition of MARCO using a ligand did not result in an increase in vomocytosis (Fig. 2G). Since polyG functions as a competitive inhibitor and likely does not block MARCO-mediated downstream signalling, this suggests that the impact of MARCO on vomocytosis can be mechanistically separated from its ligand-binding activity.

Next, we used increasing concentrations of an anti-MARCO ED31 antibody to block the activity of the MARCO receptor on wildtype macrophages. Anti-MARCO antibody reduced MARCO-mediated phagocytosis in a dose-dependent manner (Fig. 2H), without impacting the rate of vomocytosis in wildtype macrophages (Fig. 2I). According to the manufacturers, the anti-MARCO ED31 antibody recognises the ligand binding domain of MARCO receptors and can therefore compete for receptor binding with *C. neoformans* without impacting intracellular MARCO signalling [20]. Taken together, these data suggest that the role of MARCO in vomocytosis is most likely independent of its role in uptake, hence the inability of inhibitors that act on the ligand binding site to phenocopy the genetic knockout of MARCO receptor.

There is a noticeable difference in actin morphology between wildtype and *Marco*$^{-/-}$ macrophages, but "actin cage" formation is not altered

Granucci et al. [21] identified a role for MARCO in cytoskeletal remodelling of microglial and dendritic cells. Moreover, repeated actin polymerization and depolymerisation around phagosomes containing cryptococci leading to the formation of transient actin 'cages' has been shown to prevent vomocytosis [9]. We therefore wondered whether changes in the actin cytoskeleton in MARCO-deficient macrophages may underlie the difference in vomocytosis rate. Rhodamine-conjugated phalloidin staining of uninfected and *C. neoformans* infected macrophages revealed wildtype macrophages to be more rounded and compact than MARCO-deficient macrophages, which were larger, less organised and with expansive ruffle-like structures (Fig. 3A and B, white arrows). Wildtype cells had well-formed filopodial protrusions which were present, but less prominent in *Marco*$^{-/-}$ macrophages (Fig. 3B; yellow arrows).

To investigate the interaction between MARCO, actin organisation and vomocytosis, we hypothesized that one role for MARCO may be to sense phagosomal content and prevent premature expulsion, potentially by regulating the formation of actin "cages" that have previously been showing to block phagosome fusion with the plasma membrane [9]. Therefore, we quantified the presence of actin cages from immunofluorescence images of wildtype and *Marco*$^{-/-}$ macrophages (Fig. 3Bi, blue arrows). However, we observed no difference in actin cage formation between these two cell types (Fig. 3C), although there was a trend toward decreased actin cage formation following LPS stimulation, especially in wildtype macrophages.

Since actin cage formation is dependent on the Arp2/3 protein complex, we measured the transcription of ACTR2, which codes for Arp2, using qPCR. As expected, there was no MARCO expression in *Marco*$^{-/-}$ macrophages (Fig. 3D), but the level of ACTR2 expression was indistinguishable from wildtype cells (Fig. 3E). Thus, despite the difference in actin cytoskeleton organisation

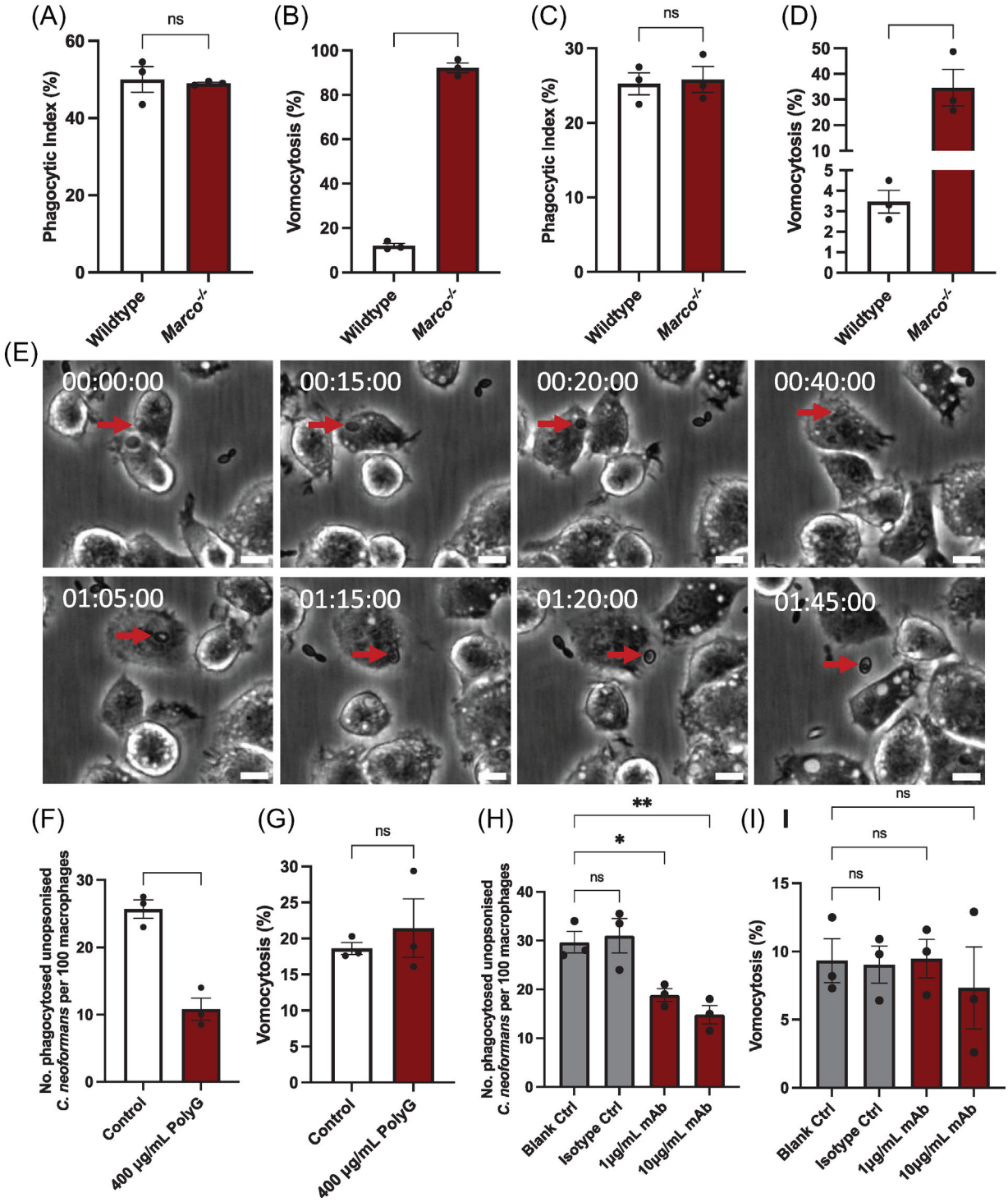

Figure 2. (A, B) Wildtype and *Marco*$^{-/-}$ macrophages were stimulated with 10 ng/mL LPS overnight, then infected with anti-GXM 18B7 antibody opsonised *C. neoformans*. After 2 h infection, images were acquired every 5 min for 16 h. (B) Wildtype: $n = 27$ vomocytosis events out of 220 infected macrophages; *Marco*$^{-/-}$: $n = 153$ vomocytosis events out of 166 infected macrophages. (C, D) LPS-stimulated macrophages were infected with a yeast-locked TetO-NRG1 *C. albicans* strain. Images were acquired every 5 min for 6 h. The phagocytic index (%) represents the percentage of macrophages that phagocytosed one or more fungal cells. At least 200 macrophages were observed per condition. Vomocytosis (%) is the percentage of infected macrophages that experienced at least one expulsion event. (D) Wildtype: $n = 4$ vomocytosis events out of 112 infected macrophages; *Marco*$^{-/-}$: $n = 36$ vomocytosis events out of 101 infected macrophages. (E) Representative image showing vomocytosis of *C. albicans* from *Marco*$^{-/-}$ MPI cells. Time is presented in hh:mm:ss; red arrows follow the course of a vomocytosis event; scale bar = 10 µm. (F, G) Wildtype macrophages were stimulated overnight with 10 ng/mL LPS. The following day, cells were pre-treated with polyguanylic acid (polyG) or (H, I) anti-MARCO ED31 monoclonal antibody (mAb) for 30 min then infected with non-opsonised *C. neoformans* still in the presence of polyG or anti-MARCO mAb. Images were acquired every 5 min for 16 h. Phagocytosis was quantified as the total number of internalised fungi per 100 macrophages at the beginning of the

between wildtype and *Marco*$^{-/-}$ macrophages, elevated vomocytosis in MARCO-deficient cells is not a consequence of altered actin cage dynamics specifically, although this does not rule out the involvement of some other actin-mediated mechanism.

Marco$^{-/-}$ cells show altered transcription of vomocytosis-relevant regulators

To date, only a handful of proteins have been demonstrated to impact vomocytosis rates, and none to the level that we report here for *Marco*$^{-/-}$ macrophages. We tested whether the loss of MARCO may lead to altered levels of these other vomocytosis-regulators by quantifying the transcription of ERK5 and ANXA2. ERK5 activity has been implicated in disruptions in the actin cytoskeleton during oncogenic transformation [22] and is known to modulate vomocytosis [12]. Additionally, MARCO may be upstream of ANXA2, another host signalling molecule found to modulate vomocytosis [13]. Annexin A2 also plays a significant role in a range of cellular processes including exocytosis and binding to actin to modulate cytoskeleton arrangement [23], processes that have been linked to nonlytic expulsion.

Interestingly, we observed elevated ERK5 expression (Fig. 3F) but reduced ANXA2 expression (Fig. 3G) in *Marco*$^{-/-}$ cells relative to wildtype cells. In both cases, this is the opposite of what might have been expected, since ERK5 acts to inhibit vomocytosis [12] and ANXA2 to stimulate it [13]. One possible interpretation is that *Marco*$^{-/-}$ cells are attempting to compensate for the uncontrolled rate of vomocytosis by altering levels of other regulators of this process. Either way, however, it is clear that accelerated non-lytic expulsion from *Marco*$^{-/-}$ cells is not mediated through ERK5/ANXA2 signalling.

Data limitations and perspectives

We have shown that loss of MARCO expression in a non-transformed GM-CSF-dependent cell line results in uncontrolled vomocytosis of *C. neoformans*. However, we have not explored whether this phenotype is replicated in a different cell line or in primary cells. In particular, it will be of considerable importance to test whether loss of MARCO induces a similar effect in the human immune system. We note also that the near-100% expulsion exhibited by *Marco*$^{-/-}$ macrophages opens the door to hitherto unfeasible approaches, such as high-throughput screening for vomocytosis inhibitors, or visualisation of vomocytosis in vivo using *Marco*$^{-/-}$ mice. Investigation into the mechanism and consequences of vomocytosis has been hindered by its rarity in vitro and the need to observe the phenomenon using live cell imaging. Our finding with *Marco*$^{-/-}$ macrophages offers much-needed solution to one of these challenges, which we hope will invite further experimentation into this outcome of *C. neoformans* infection.

Conclusion

Here we present a novel role for MARCO in modulating the vomocytosis of *C. neoformans*. The increase in vomocytosis observed in *Marco*$^{-/-}$ macrophages is the most dramatic change in vomocytosis rate observed to date. Increased vomocytosis in *Marco*$^{-/-}$ macrophage was also observed when macrophages were infected with a yeast-locked *C. albicans* strain, suggesting that MARCO's modulation of vomocytosis is a broadly relevant phenomenon. Given that MARCO deficiency still resulted in elevated vomocytosis of antibody-opsonised *C. neoformans* and *C. albicans*, we propose that MARCO's role in vomocytosis is independent of the mode of uptake, and instead that MARCO may modulate vomocytosis through a yet to be identified mechanism. Finally, we note that this hitherto undocumented impact of MARCO loss on pathogen expulsion will be important for investigators to consider when using *Marco*$^{-/-}$ cells or animals for a range of other infection assays.

Materials and methods

Max Planck Institute cell culture

Max Planck Institute (MPI) cells are a non-transformed, GM-CSF-dependent murine macrophage cell line that is functionally similar to alveolar macrophages [15, 24]. MPI cell lines isolated from wildtype and MAcrophage Receptor with COllagenous structure knockout (*Marco*$^{-/-}$) mice were cultured in Roswell Park Memorial Institute (RPMI) 1640 medium [ThermoFisher] supplemented with 10% heat-inactivated FBS (Sigma-Aldrich), 2 mM L-glutamine (Sigma-Aldrich), and 1% Penicillin and Streptomycin solution (Sigma-Aldrich) at 37°C and 5% CO_2. Each flask was further supplemented with 1% vol/vol GM-CSF conditioned RPMI media prepared using an X-63-GMCSF cell line.

Phagocytosis assay

Twenty-four hours before the start of the phagocytosis assay, MPI cells were seeded onto 24-well plates at a density of 2×10^5 cells/mL in complete culture media supplemented with 1%

timelapse video. (G) Control: $n = 34$ vomocytosis events out of 183 infected macrophages; PolyG treated: $n = 34$ vomocytosis events out of 160 infected macrophages. (I) Blank Ctrl: $n = 15$ vomocytosis events out of 154 infected macrophages; isotype Ctrl: $n = 13$ vomocytosis events out of 143 infected macrophages; 1 μg/mL mAb: $n = 11$ vomocytosis events out of 117 infected macrophages; 10 μg/mL mAb: $n = 7$ vomocytosis events out of 100 infected macrophages. Data is representative of at least two independent experiments. Data shown as mean ± SEM; ns, not significant; $^*p < 0.05$; $^{**}p < 0.01$, $^{****}p < 0.0001$ in an unpaired two-sided *t*-test (A–D, F–G) or one-way ANOVA followed by Tukey's post hoc test (H, I).

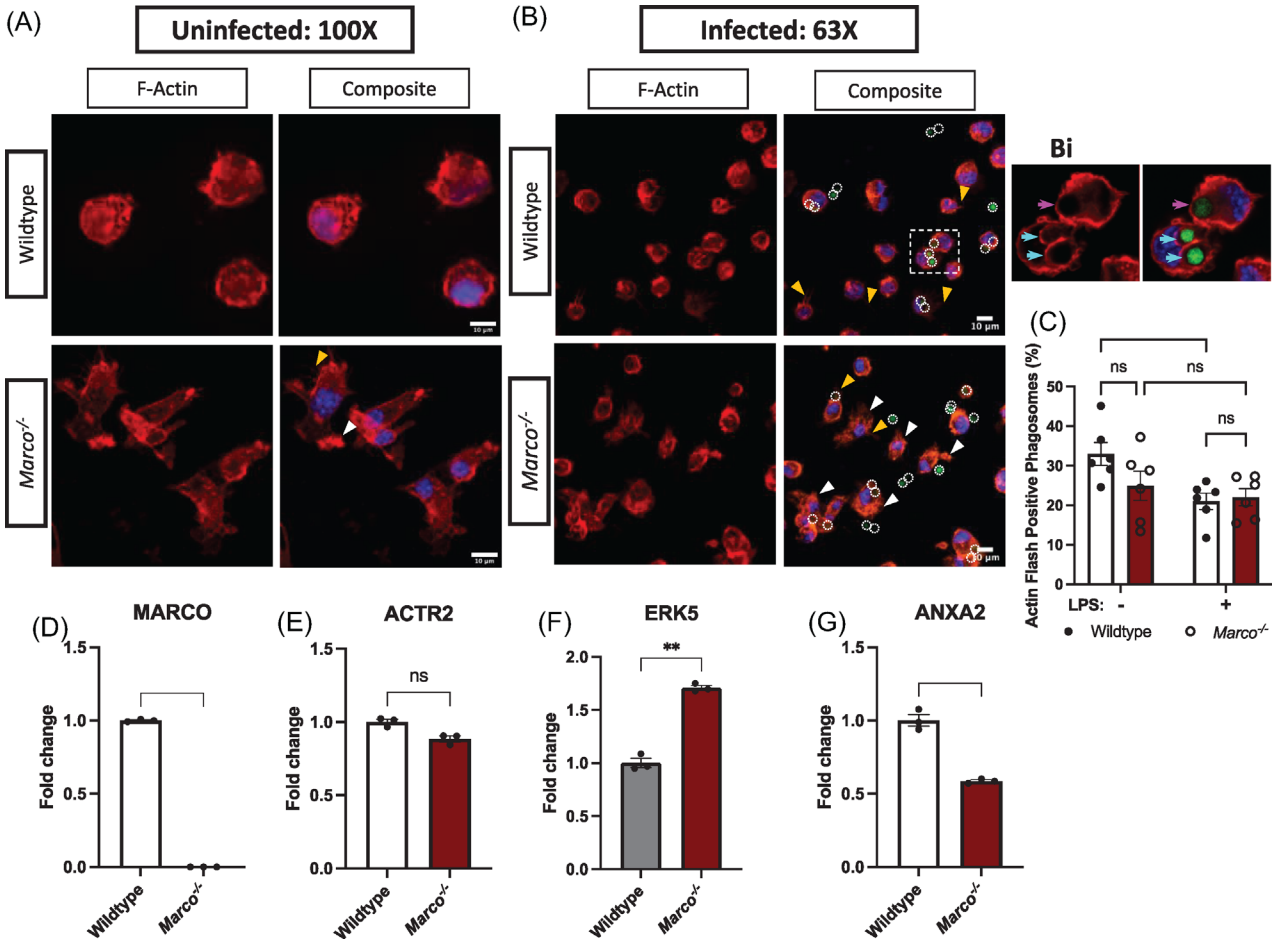

Figure 3. Wildtype and *Marco*$^{-/-}$ macrophages were stimulated with 10 ng/mL LPS overnight, left uninfected (A) or infected with non-opsonised GFP-expressing *C. neoformans* for 2 h (B). Following 2 h infection, macrophages were fixed and permeabilized, and F-actin was stained with rhodamine-conjugated phalloidin. Cells were counter-stained with DAPI to visualize the nucleus, then mounted onto glass slides using Fluoromount mounting medium. Z-stack images were acquired using the Zeiss LSM880 confocal microscope using 100X Oil (A) and 63X Oil magnification (B). Z-stack maximum intensity projection was applied to the images. Red = F-actin (Phalloidin); Blue = Nucleus; Green with white dashed circle = *C. neoformans*. White arrows show examples of macrophages with ruffle-like structures; Yellow arrows show examples of filopodial protrusions. Scale bar = 10 μm. (Bi) Represents 2× zoom of area in (B) marked with a white dashed box without maximum intensity projection applied. Blue arrows show presence of actin cage/flash around internalised *C. neoformans*. Pink arrow shows phagosome without actin cage/ flash. (C) The percentage of actin flash-positive phagosomes were quantified from fluorescent microscopy images. Data pooled from two independent experiments. Expression of MARCO (D), ACTR2 (E), ERK5 (F), and ANXA2 (G) was measured using reverse transcription quantitative PCR. The fold change in gene expression was quantified using the $2-\Delta\Delta Ct$ method. (C–G) Data are shown as mean ± SEM; ns, not significant; $^{*}p < 0.05$; $^{**}p < 0.01$, $^{****}p < 0.0001$ in a two-way ANOVA followed by Tukey's post hoc test (C) or a paired two-sided *t*-test (D–G).

vol/vol GM-CSF. The cells were then incubated overnight at 37°C and 5% CO_2. The following day, macrophages were stimulated with 10 ng/mL LPS from *Escherichia coli* (Sigma-Aldrich; cat#: L6529) and 1% vol/vol GM-CSF for 24 h. At the same time, an overnight culture of *C. neoformans* var. *grubii* KN99α strain, which had previously been biolistically transformed to express GFP [25], was set up by picking a fungal colony from YPD agar plates (50 g/L YPD broth powder [Sigma-Aldrich], 2% Agar [MP Biomedical]) and resuspending in 3 mL liquid YPD broth (50 g/L YPD broth powder [Sigma-Aldrich]). The culture was then incubated at 25°C overnight under constant rotation (20 rpm).

After overnight LPS stimulation, macrophages were infected with non-opsonised *C. neoformans*. To prepare *C. neoformans* for infection, an overnight *C. neoformans* culture was washed two times in 1X PBS, counted using a haemocytometer, and fungi incubated with macrophages at an MOI of 10:1. The infection was allowed to proceed for 2 h at 37°C and 5% CO_2 before starting timelapse imaging. Meanwhile, to follow infection from uptake through to vomocytosis, timelapse imaging began immediately following macrophage incubation with *C. neoformans* at an MOI 0.5:1.Where applicable, macrophages were pre-treated with 400 μg/mL polyG (Sigma-Aldrich; cat#: P4404), rat anti-mouse MARCO ED31 clone monoclonal antibody (BioRad; Cat#: MCA1849), or anti-rat IgG1 isotype control (Invitrogen; cat#: 14430182) for 30 min at 37°C prior to 2 h infected with non-opsonised *C. neoformans*. In these cases, prior to timelapse imaging and after washing off extracellular *C. neoformans*, polyG ligand or anti-MARCO antibodies were added back into the wells.

Table 3. List of primers used in RT-qPCR.

	Forward primer	Reverse primer
MARCO	ACAGAGCCGATTTTGACCAAG	CAGCAGTGCAGTACCTGCC
ANXA2	CACCAACTTCGATGCTGAGAGG	GCACATTGCTGCGGTTTGTCAG
ACTR2	CACAATCCAGGCAGCCGACATT	AGCTCTCGTTCCAACCTCGATG
ERK5	CAGCCTTCTACATCAGAGTCACC	CCTTTGGAGTGCCAGAGAACAC
TBP	CTACCGTGAATCTTGGCTGTAAAC	AATCAACGCAGTTGTCCGTGGC

For infection with antibody-opsonised *C. neoformans*, 1×10^6 yeast cells in 100 μL PBS were opsonized for 1 h using 10 μg/mL anti-capsular 18B7 antibody (a kind gift from Arturo Casadevall, Albert Einstein College of Medicine). For infection with heat-killed *C. neoformans*, fungi were killed by heating at 56°C for 30 min. After 2 h infection at 37°C, macrophages were washed four times with PBS to remove as much extracellular *C. neoformans* as possible, then used for live imaging.

To explore the vomocytosis of *Candida albicans*, a yeast-locked *C. albicans* strain was used (a kind gift from Hung-Ji Tsai, University of Birmingham). The yeast-locked TetOn-NRG1 *C. albicans* strain constitutively expresses the Nrg1 transcription factor, thereby preventing yeast to hypha transition [16]. A colony was suspended in 10 mL YPD broth and incubated overnight at 30°C and 180 rpm. Prior to their use in infection, a *C. albicans* overnight culture was diluted 1:100 in fresh YPD broth, then incubated at 30°C and 180 rpm for 3 h till cells were in the exponential phase. Cells in the exponential phase were washed with PBS and counted, and macrophages were infected at MOI 2:1. For infection with *C. albicans*, imaging began immediately following infection.

Time-lapse imaging

Live-cell imaging was performed using a Zeiss Axio Observer [Zeiss Microscopy] or Nikon Eclipse Ti (Nikon) at 20× magnification. Images were acquired every 5 min for 16 h at 37°C and 5% CO_2. The resulting videos were analysed using Fiji (ImageJ), at least 200 macrophages were observed, and vomocytosis was scored according to the following guideline described previously [12]:

1. One vomocytosis event is the expulsion of internalized cryptococci from an infected macrophage, regardless of the number of cryptococci expelled if they do so simultaneously.
2. Vomocytosis events are scored as independent phenomena if they occur in different frames or from different macrophages.
3. Vomocytosis events are discounted if the host macrophage subsequently undergoes lysis or apoptosis within 30 min.

Vomocytosis was presented as the percentage of infected macrophages that experienced one or more vomocytosis events. For non-opsonic uptake of *C. neoformans*, phagocytosis was presented as the number of internalised cryptococci per 100 macrophages, since individual internalised fungi can be accurately delineated. Meanwhile, phagocytosis of antibody opsonised *C. neoformans* and *C. albicans* was presented as the percentage of macrophages that phagocytosed at least one fungal cell (phagocytic index (%)) due to the more efficient phagocytosis of these cells by macrophages.

F-Actin staining and confocal microscopy

Macrophages were seeded on 13 mm coverslips placed into 24-well plates. Staining was performed on macrophages fixed with 4% paraformaldehyde for 10 min at room temperature and permeabilised with 0.1% Triton X-100 diluted in PBS for 10 min at room temperature. F-actin filaments were stained using two units of rhodamine-conjugated phalloidin stain (Invitrogen; cat#: R415) diluted in 400 μL 1% BSA in 1X PBS and incubated for 20 min at room temperature. Cells were washed with PBS, then counter-stained with 0.5 μg/mL DAPI for 5 min at room temperature to visualize the nucleus. After PBS washes, glass slides were mounted using Fluoromount mounting medium (Sigma; cat#: F4680). Z-stack images were acquired using the Zeiss LSM880 Confocal with Airyscan2, laser lines 405, 488, 561, and 640 nm, and at 63× or 100× oil magnification. Image acquisition was performed using the ZEN Black software (Zeiss Microscopy) and the resulting images were analysed using the Fiji image processing software (ImageJ).

Quantitative reverse transcription PCR

Total RNA was exacted from cell lines using RNeasy kit (Qiagen). The concentration of RNA was measured on a NanoDrop spectrophotometer, and reverse transcription was performed using the high-capacity cDNA reverse transcription kit (Applied Biosystems) according to the manufacturer's instructions. Quantitative PCR (qPCR) was performed on the QuantStudio 7 real-time PCR system (ThermoFisher) and the Power SYBR Green PCR Master Mix (Applied Biosystems). The relative fold changes in gene expression were determined using the $2-\Delta\Delta Ct$ method and normalized to the expression of TBP. The list of primers used can be found in Table 3.

Statistics

GraphPad Prism Version 9 for Mac (GraphPad Software) was used to generate graphical representations of experimental data. Violin

plots were generated using R programming. Inferential statistical tests were performed using Prism. The data sets were assumed to be normally distributed based on results of Shapiro–Wilk test for normality. Consequently, to compare the means between treatments, the following parametric tests were performed: unpaired two-sided *t*-test, one-way ANOVA followed by Tukey's post hoc test. When data failed the normality test, the Mann–Whitney *U* nonparametric test was used. Variation between treatments was considered statistically significant if P-value < 0.05.

Acknowledgements: The authors thank Hung-Ji Tsai for the provision of yeast-locked *C. albicans* strain. C.U.O is supported by a PhD studentship from the Darwin Trust of Edinburgh. Gyorgy Fejer acknowledges funding from the NC3Rs (grant number NC/V001019/1). Robin C. May gratefully acknowledges support from the BBSRC and the European Research Council Consolidator Award.

Conflict of interest: All authors declare no commercial or financial conflict of interest.

Author Contributions: Chinaemerem U. Onyishi and Robin C. May generated hypotheses and designed the experiments. Chinaemerem U. Onyishi performed most the experiments, analysed the data and wrote the manuscript. Yusun Jeon performed qRT-PCR experiment and analysed the data. Subhankar Mukhopadhyay, Siamon Gordon and Gyorgy Fejer provided Wildtype and *Marco*$^{-/-}$ MPI cells and provided a critical discussion of the experimental results. Robin C. May acquired funding. All authors contributed to the review of the manuscript.

Data Availability Statement: The data that support the findings of this study are available from the corresponding author upon reasonable request.

Peer review: The peer review history for this article is available at https://publons.com/publon/10.1002/eji.202350771

References

1 **May, R. C., Stone, N. R. H., Wiesner, D. L., Bicanic, T. and Nielsen, K.**, Cryptococcus: from environmental saprophyte to global pathogen. *Nat Rev Microbiol*. 2016. **14**: 106–117.

2 **Gilbert, A. S., Wheeler, R. T. and May, R. C.**, Fungal pathogens: survival and replication within macrophages. *Cold Spring Harb Perspect Med*. 2015. **5**: a019661.

3 **Ma, H., Croudace, J. E., Lammas, D. A. and May, R. C.**, Direct cell-to-cell spread of a pathogenic yeast. *BMC Immunol*. 2007. **8**: 15.

4 **Alvarez, M. and Casadevall, A.**, Cell-to-cell spread and massive vacuole formation after *Cryptococcus neoformans* infection of murine macrophages. *BMC Immunol*. 2007. **8**: 16.

5 **Johnston, S. A. and May, R. C.**, Cryptococcus interactions with macrophages: evasion and manipulation of the phagosome by a fungal pathogen. *Cellular Microbiology*. 2013. **15**: 403–411.

6 **Ma, H., Croudace, J. E., Lammas, D. A. and May, R. C.**, Expulsion of live pathogenic yeast by macrophages. *Current Biology*. 2006. **16**: 2156–2160.

7 **Alvarez, M. and Casadevall, A.**, Phagosome extrusion and host-cell survival after *Cryptococcus neoformans* phagocytosis by macrophages. *Current Biology*. 2006. **16**: 2161–2165.

8 **Seoane, P. I. and May, R. C.**, Vomocytosis: what we know so far. *Cellular Microbiology*. 2019. **22**: e13145.

9 **Johnston, S. A. and May, R. C.**, The human fungal pathogen cryptococcus neoformans escapes macrophages by a phagosome emptying mechanism that is inhibited by Arp2/3 complex-mediated actin polymerisation. *PLOS Pathogens*. 2010. **6**: e1001041.

10 **Smith, L. M., Dixon, E. F. and May, R. C.**, The fungal pathogen Cryptococcus neoformans manipulates macrophage phagosome maturation. *Cellular Microbiology*. 2015. **17**: 702–713.

11 **Fu, M. S., Coelho, C., De Leon-Rodriguez, C. M., Rossi, D. C. P., Camacho, E., Jung, E. H., Kulkarni, M., et al.**, Cryptococcus neoformans urease affects the outcome of intracellular pathogenesis by modulating phagolysosomal pH. May, RC, editor. *PLoS Pathog*. 2018. **14**: e1007144.

12 **Gilbert, A. S., Seoane, P. I., Sephton-Clark, P., Bojarczuk, A., Hotham, R., Giurisato, E., Sarhan, A. R., et al.**, Vomocytosis of live pathogens from macrophages is regulated by the atypical MAP kinase ERK5. *Sci Adv*. 2017. **3**: e1700898.

13 **Stukes, S., Coelho, C., Rivera, J., Jedlicka, A. E., Hajjar, K. A. and Casadevall, A.**, The membrane phospholipid binding protein annexin A2 promotes phagocytosis and non-lytic exocytosis of *Cryptococcus neoformans* and impacts survival in fungal infection. *J Immunol*. 2016. **197**: 1252–1261.

14 **Seoane, P. I., Taylor-Smith, L. M., Stirling, D., Bell, L. C. K, Noursadeghi, M., Bailey, D. and May, R. C.**, Viral infection triggers interferon-induced expulsion of live *Cryptococcus neoformans* by macrophages. *PLOS Pathogens*. 2020. **16**: e1008240.

15 **Fejer, G., Wegner, M. D., Györy, I., Cohen, I., Engelhard, P., Voronov, E., Manke, T, et al.**, Nontransformed, GM-CSF–dependent macrophage lines are a unique model to study tissue macrophage functions. *Proc Natl Acad Sci USA.* 2013. **110**: E2191–E2198.

16 **Ost, K. S., O'Meara, T. R., Stephens, W. Z., Chiaro, T., Zhou, H., Penman, J., Bell, R., et al.**, Adaptive immunity induces mutualism between commensal eukaryotes. *Nature*. 2021. **596**: 114–118.

17 **Gantner, B. N., Simmons, R. M. and Underhill, D. M.**, Dectin-1 mediates macrophage recognition of *Candida albicans* yeast but not filaments. *EMBO J*. 2005. **24**: 1277–1286.

18 **Bain, J. M., Lewis, L. E., Okai, B., Quinn, J., Gow, N. A. R and Erwig, L. P.**, Non-lytic expulsion/exocytosis of *Candida albicans* from macrophages. *Fungal Genet Biol*. 2012. **49**: 677–678.

19 **Kanno, S., Hirano, S., Sakamoto, T., Furuyama, A., Takase, H., Kato, H., Fukuta, M, et al.**, Scavenger receptor MARCO contributes to cellular internalization of exosomes by dynamin-dependent endocytosis and macropinocytosis. *Sci Rep*. 2020. **10**: 21795.

20 **van der Laan, L. J. W, Döpp, E. A., Haworth, R., Pikkarainen, T., Kangas, M., Elomaa, O., Dijkstra, C. D., et al.**, Regulation and functional involvement of macrophage scavenger receptor MARCO in clearance of bacteria in vivo. *The Journal of Immunology*. 1999. **162**: 939–947.

21 **Granucci, F., Petralia, F., Urbano, M., Citterio, S., Di Tota, F., Santambrogio, L. and Ricciardi-Castagnoli, P**, The scavenger receptor MARCO mediates

cytoskeleton rearrangements in dendritic cells and microglia. *Blood*. 2003. **102**: 2940–2947.

22 **Barros, J. C. and Marshall, C. J.**, Activation of either ERK1/2 or ERK5 MAP kinase pathways can lead to disruption of the actin cytoskeleton. *Journal of Cell Science*. 2005. **118**: 1663–1671.

23 **Gabel, M. and Chasserot-Golaz, S.**, Annexin A2, an essential partner of the exocytotic process in chromaffin cells. *Journal of Neurochemistry*. 2016. **137**: 890–896.

24 **Maler, M. D.**, **Nielsen, P. J.**, **Stichling, N.**, **Cohen, I.**, **Ruzsics, Z.**, **Wood, C.**, **Engelhard, P.**, **et al.** Key role of the scavenger receptor MARCO in mediating adenovirus infection and subsequent innate responses of macrophages. *mBio*. 2017. **8**: e00670–e00717.

25 **Voelz, K.**, **Johnston, S. A.**, **Rutherford, J. C. and May, R. C.**. Automated analysis of cryptococcal macrophage parasitism using GFP-tagged Cryptococci. *PLOS ONE*. 2010. **5**: e15968.

Abbreviations: **ANXA2:** Annexin A2 · **MARCO:** MAcrophage Receptor with COllagenous domain · **polyG:** polyguanylic acid potassium salt · **qPCR:** quantitative PCR

Full correspondence: Dr. Chinaemerem U. Onyishi and Prof. Robin C. May, Institute of Microbiology & School of Biosciences, University of Birmingham, Edgbaston, Birmingham, B15 2TT, United Kingdom
e-mail: chinaemerem.onyishi@nih.gov and r.c.may@bham.ac.uk

Received: 12/9/2023
Revised: 3/3/2024
Accepted: 5/3/2024
Accepted article online: 7/3/2024